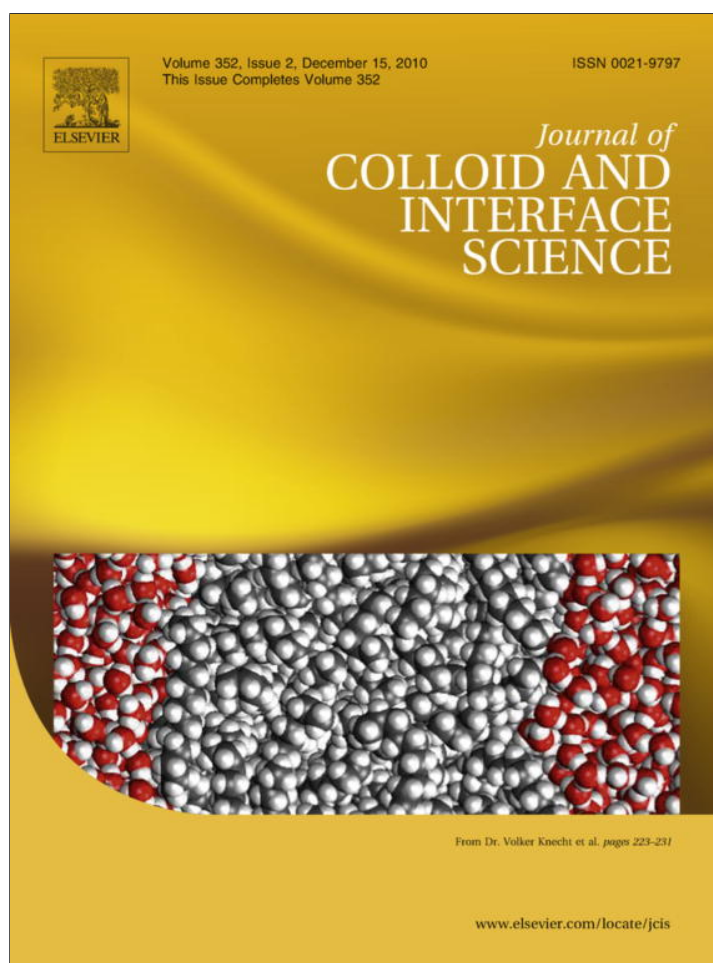


Provided for non-commercial research and education use.
Not for reproduction, distribution or commercial use.



This article appeared in a journal published by Elsevier. The attached copy is furnished to the author for internal non-commercial research and education use, including for instruction at the authors institution and sharing with colleagues.

Other uses, including reproduction and distribution, or selling or licensing copies, or posting to personal, institutional or third party websites are prohibited.

In most cases authors are permitted to post their version of the article (e.g. in Word or Tex form) to their personal website or institutional repository. Authors requiring further information regarding Elsevier's archiving and manuscript policies are encouraged to visit:

<http://www.elsevier.com/copyright>



Contents lists available at ScienceDirect

Journal of Colloid and Interface Science

www.elsevier.com/locate/jcis



Adsorption of surfactant-rich stickies onto mineral surfaces

Christopher M. Gribble^a, G. Peter Matthews^{a,*}, Daniel Gantenbein^{a,b}, Andrew Turner^a, Joachim Schoelkopf^b, Patrick A.C. Gané^{b,c}^a School of Geography, Earth and Environmental Sciences, University of Plymouth, Drake Circus, Plymouth PL4 8AA, UK^b Omya Development AG, CH-4665 Oftringen, Switzerland^c Aalto University, School of Science and Technology, Faculty of Chemistry and Materials Sciences, Department of Forest Products Technology, P.O. Box 16300, 00076 Aalto, Finland

ARTICLE INFO

Article history:

Received 31 March 2010

Accepted 24 July 2010

Available online 3 August 2010

Keywords:

Adsorption

Calcium carbonate

Paper recycling

Stickies

Talc

ABSTRACT

“Stickies” are tacky species, present in recycled paper and coated broke, derived from coating formulations, adhesives etc. They impact negatively on paper quality and cause web runnability problems by deposit build-up. To sustain recycling, stickies are controlled by adsorbing them onto minerals added to the recycled stock. We report isotherms for a fatty acid ester defoamer and an acrylic acid ester copolymer adsorbing from colloidal suspension onto various talcs and modified calcium carbonates. We used commercial preparations of the fatty acid ester defoamer and acrylic acid ester copolymer to provide a simple analogue to the industrial process. The modified calcium carbonates are hydrophilic with anionic and cationic sites present. Adsorption isotherms for low surface area modified calcium carbonate conform to the Langmuir model, while those for high surface area modified calcium carbonate reflect a two stage process involving the formation of a monolayer over the mineral surface and subsequent partial aggregation. Talc platelets display hydrophilic edges and hydrophobic surfaces. Adsorption onto them appears to involve three stages; specifically, a hydrophilic interaction between hydrophilic groups on the molecules and the talc edges, followed by hydrophobic interactions between the molecules and the talc surfaces, and finally by formation of multilayers.

© 2010 Published by Elsevier Inc.

1. Introduction

There continues to be considerable environmental pressure to increase the use of recycled paper, but its use is not without complications. Some of the most difficult problems result from the presence of adhesives, arising from hot melt glues, binders and other thermoplastic materials, for example from book-backs and adhesive tape or from silicone based defoamers. They tend to be pliable organic materials, such as styrene-butadiene and styrene acrylic latex binders, rubber, vinyl acrylates, polyisoprene, polybutadiene and hot melts [1–4]. Under certain conditions, these compounds can become tacky and deposit as ‘stickies’ in the paper machine. Stickies have multiple deleterious effects on paper quality including sheet indentations, sheet structural defects, web breaks, and discolouration such as black spots [5–7]. The correction of these faults increases production costs.

Once stickies are released by the pulping process, they can accumulate in the white water system of the recycled fibre section of a paper recycling mill. Similarly, fibre stock containing recycled fibre can suffer from a build-up of stickies on the paper making machine. As paper mills are continuing to reduce their fresh water usage to minimise costs, white water recycling is becoming more

prevalent, increasing the concentration of stickies and thus making them even more problematic.

Studies of stickies that have been reported in the literature are mainly concerned with how the effects of these compounds may be reduced in paper mills [5,8], or the development of alternative paper additives that have less of a detrimental effect during paper recycling [8,9]. Some studies focus on the removal of stickies and pitch from the recycled fibre system by, for example, screening [10–12], flotation [11,13,14] and adsorption [15–17], or from the white water in the paper mill [18,19]. Stickies are classified by size and how they are introduced into the system, as defined in Table S1 of the Supplementary information [20].

To remove stickies from the white water system, it is possible to adsorb them onto a mineral surface, and then incorporate the mineral and adsorbate into the paper structure, thus transporting the stickies out of the machine within the final product. The aim of this investigation was to define the extent and nature of adsorption of stickies onto various contrasting mineral surfaces. Because of the colloidal nature of the adsorbent and inexact knowledge of the commercially-supplied model stickies and surfactants, the isotherms and other measurements all refer to operationally-defined conditions. However, the general approach and interpretation is applicable to other systems in which species in aqueous colloidal suspension adsorb onto suspended solid particles.

* Corresponding author. Fax: +44 0 1752 584790.

E-mail address: pmatthews@plymouth.ac.uk (G.P. Matthews).

The adsorption measurements presented here involve colloidal species with hydrophilic and hydrophobic regions, stabilised in aqueous solution by unknown quantities of surfactant, adsorbing onto hydrophilic and hydrophobic mineral surfaces. The adsorption conditions of the experiment allow more than one adsorption mechanism to exist. In order to understand the processes that occurred, it was decided to fit the experimental data with simple Langmuir gas-adsorption isotherms relating to these operationally-defined colloidal conditions. Langmuir isotherms assume single layer, localised adsorption with identical interaction energies for each adsorbed molecule [21]. The adsorption interactions studied in this work are much more complicated, but nevertheless fitting of the Langmuir isotherm to individual adsorption stages provides a convenient method of smoothing and quantifying the measurements, and of calculating asymptotes.

The adsorption of a typical surfactant onto a solid/liquid surface can be divided into four stages [25]. The first stage, in which individual isolated species adsorb by electrostatic interaction, obeys the Gouy–Chapman equation [26] (or Henry's Law [27]) with adsorption increasing linearly with concentration [25]. At the onset of the second stage, surfactant species start to associate with lateral electrostatic interactions to form hemimicelles etc. This lateral interaction causes a sharp increase in adsorption density, which can be studied using an isotherm appropriate for monolayer formation. The third adsorption stage can be analysed using a bilayer isotherm [27]. The fourth stage is the desorption of surfactants [28].

We have fitted the monolayer formation stages (I and II) to a form of the Dubinin–Radushkevich (D–R) equation adapted for adsorption in aqueous systems [22,23]:

$$q_e = q_d \exp \left(- \left(\frac{1}{2E^2} \right) \left[RT \ln \left(1 + \frac{1}{c_e} \right) \right]^2 \right) \quad (1)$$

Here q_e is the adsorbed concentration at equilibrium on the surface of the mineral, R is the universal gas constant, T is the absolute temperature, E the free energy of sorption per mole of the sorbate, c_e the aqueous equilibrium concentration, and q_d the D–R isotherm constant. A plot of $\ln q_e$ against $RT \ln(1 + 1/c_e)$ yields E and q_d . An adsorption energy E of less than 5 kJ mol^{-1} implies physisorption, whereas a value greater than 10 kJ mol^{-1} implies chemisorption [24].

For adsorption of surfactants, a finite number of layers of surfactant may form on the surface [27], whereas BET theory allows formation of an unlimited number of layers [29,30]. A new 'ARIAN' (adsorption isotherms regional analysis) equation was derived by Samiey to study bilayer isotherms [27], Eq. (2). (There are alternate forms of this equation for low bilayer coverage, Eq. S1 in the Supplementary information, and for monolayers, Eq. S2, which converge as expected to a Langmuir-type equation.)

$$q_e = c_e \left(\frac{q_{\text{mon}} K_{\text{sa}} + 2q_{\text{mon}} \chi c_e K_{\text{sa}}}{1 + c_e K_{\text{sa}} + \chi c_e^2 K_{\text{sa}}} \right) \quad (2)$$

Here, q_{mon} is the monolayer adsorption capacity, K_{sa} is an equilibrium constant of surfactant molecules in surface aggregates of the primary layer, and χ is an equilibrium constant of surfactant molecules in surface aggregates in all layers above the first.

Non-ionic surfactants are also able to form surface aggregates, e.g. when adsorbing onto silica-gel, and the adsorption of non-ionic surfactants is normally reversible with little hysteresis. The surfactants are unable to adsorb onto some mineral surfaces such as alumina because the surfactant is unable to disrupt the rigid water layer surrounding the substrate. They use hydrogen bonding to adsorb onto the surface, which is relatively weak in comparison with electrostatic and chemical bonds [26,45].

Talc, $\text{Mg}_3\text{Si}_4\text{O}_{10}(\text{OH})_2$, is a phyllosilicate consisting of a magnesium hydroxide layer ($\text{MgO} \cdot \text{H}_2\text{O}$) sandwiched by two silicate layers (SiO_2) forming a three layer structure. Van der Waals forces hold the adjacent layers together weakly, giving talc a platy and readily delaminating morphology. The edges of the talc are predominantly hydrophilic hydroxide groups [31], whereas the talc faces are largely silicate. The absence of surface charge on the silicate layers renders the surface more attractive to air than to water, and it is the retention of a suspected air layer [32] when suspended in water that allows the platelet surface to undergo hydrophobic interactions [33].

We define 'aspect ratio' as the ratio of the largest dimension of the mineral particle relative to the smallest dimension. In the case of a platelet, such as found in talc, the largest axis is the diametrical dimension, related to the platelet planar surface, and the smallest that of the platelet edge thickness. The aspect ratio varies for different grades of talc, and the larger the aspect ratio, the greater the ratio of hydrophobic to hydrophilic surface area.

Modified calcium carbonates [34] (MCC) are formed from calcium carbonate treated with phosphoric acid, citric acid or a combination of similar acids to provide an *in situ* surface re-precipitation of a chosen structure. (MCC is a product technology of Omya Development AG.) In this investigation, two grades of modified natural calcium carbonate were used; LSA (lower surface area) MCC and HSA (higher surface area) MCC. Scanning electron microscope (SEM) images of freeze-dried LSA MCC and HSA MCC are displayed in the Supplementary information. MCCs have hydrophilic surfaces, and each material exhibits both calcium phosphate and carbonate crystal structure as determined by X-ray powder diffraction. Mercury porosimetry of the MCC samples revealed that both have a peak in pore size at 510 nm, but that the LSA MCC is bimodal with a second peak at 91 nm.

2. Materials

2.1. Minerals

The minerals used in this investigation were talc and modified calcium carbonate, in forms that have been used in paper manufacture either as a paper coating or filler, and that are commercially available. Detailed information about the mineral preparation and suppliers is found in Supplementary information. Table 1 summarises the surface area and particle size distribution of the minerals used.

2.2. Stickies

The two stickies selected for the present study were supplied by BASF and are commercially available analogues of typical stickies found in a paper mill. The first was an acrylic acid ester copolymer (AAEC), product name Acronal V 212, and the second was a fatty acid ester defoamer (FAED) named Afranil RS. Their solid contents

Table 1
Details of minerals used in this investigation. d_N is the equivalent spherical diameter at which N w/w% of the mineral particles are finer.

Name	Specific surface area ($\text{m}^2 \text{g}^{-1}$)	Particle size-weight distribution (μm)		
		d_{10}	d_{50}	d_{90}
Low surface area talc (LSA talc)	7.13	2.24	4.50	10.1
High surface area talc (HSA talc)	45.3	1.56	5.02	21.0
Low surface area modified calcium carbonate (LSA MCC)	36.1	2.55	5.49	9.85
High surface area modified calcium carbonate (HSA MCC)	113.0	1.82	4.26	9.37

of 68.3% and 30.3%, respectively, were measured by evaporating a known weight of sticky suspension at 130 °C until constant weight was achieved. It was assumed that no volatile organic compounds were lost in the measurement of solid content. Both stickies investigated have hydrophilic and hydrophobic regions of the molecule.

3. Experimental methods

Data were derived using two analytical techniques for initial concentrations of model stickies covering the range 0.005–0.5 g dm⁻³; namely dissolved organic carbon analysis and elemental analysis.

3.1. Sticky preparation

All experiments were undertaken at room temperature (20.5 ± 1.5 °C). Both stickies were prepared to form colloidal stable suspensions in Millipore Milli-Q water with an initial dry weight concentration of 0.5 g dm⁻³. The initial pH was between 7 and 7.5 and initial conductivity was in the range of 1000–1500 μS cm⁻¹. They were adjusted to these ranges where necessary using dilute analytical grade hydrochloric acid, analytical grade sodium hydroxide and laboratory grade sodium chloride (all supplied by Thermo Fisher Scientific UK).

These sticky suspensions were then diluted in Milli-Q water to 0.1, 0.05, 0.01 and 0.005 g dm⁻³. Minerals were added to the sticky suspensions as slurries (solid contents 8–10%) to give a concentration of 1.93–2.22 g dm⁻³. The pH and conductivity were not controlled during the experiments.

Resulting suspensions were agitated for 30 min at 150 min⁻¹ on an orbital shaker before minerals with adsorbed stickies were removed by centrifuging at 2000 g for 15 min. The mineral with adsorbed sticky collected after centrifuging was freeze-dried for two days, then transferred to air-tight bags for storage (under desiccation) prior to analysis.

3.2. Dissolved organic carbon analysis

Dissolved organic carbon analysis was performed using standard operating procedures [35,36], as detailed in the [Supplementary information](#). Dissolved organic carbon (DOC) analysis was performed with a Shimadzu TOC-5000A total organic carbon analyser coupled to a Shimadzu ASI-5000 autosampler (Shimadzu Corp. Japan).

3.3. Elemental analysis

The elemental analysis was performed on a Carlo Erba EA-1110 CHNS elemental analyser, (Thermo Fisher Scientific, USA), using standard operating procedures, briefly summarised in the [Supplementary information](#).

3.4. Turbidity

The turbidity of the sticky suspensions, mineral suspensions and sticky and mineral suspensions were measured on a Hach DR/890 Colorimeter (Hach Company, USA). Turbidity is a measure of light scattering by particles in suspension. The particle size distribution of the scattering particles is a key factor in altering the turbidity of the suspension [37]. The turbidity (τ) is proportionally related to the numerical particle concentration (c') and volume (v) of the scattering particles, Eq. (3).

$$\tau \propto v^2 c' = (vc')v \quad (3)$$

If species aggregate, the volume v of the individual aggregates will increase while the number concentration (c') of the aggregates

will decrease proportionally. Therefore, the term (vc') will remain constant, and the turbidity τ is directly proportional to the volume v of the aggregates.

3.5. Zeta potential

The zeta potential of the 0.5 g dm⁻³ sticky suspensions was measured on a Zetasizer Nano (Malvern Instruments Ltd., UK.) before the mineral was added, and after the mineral with adsorbate was removed by centrifugation. The zeta potential gave a measure of the coulombic stability of the colloidal suspensions, and how the stability of the remaining suspension changed because of the adsorption of sticky onto mineral surfaces. A change in magnitude of the zeta potential was also useful in determining if cationic or anionic species were adsorbed preferentially [38].

3.6. Data presentation and analysis

Dissolved organic carbon analysis gave the carbon content remaining in solution after adsorption of the sticky had occurred and the mineral had been removed by centrifuging. The equilibrium carbon concentration on the surface of the mineral was determined by elemental analysis. The elemental analysis results were normalised to allow for the change in mass encountered because of adsorption of the fatty acid ester defoamer and acrylic acid ester copolymer. The elemental analysis results have also been corrected for the carbon content found in the minerals themselves.

The values are obtained using two techniques which are independent of each other. It is also possible to convert the carbon values into absolute values of sticky concentration using a calibration series of dissolved organic carbon measurements, and then using mass balance calculations for the concentrations of the species adsorbed onto the surfaces. However, once presented in this way, the variables are no longer independent of each other, so we have not used this method of data analysis in this work.

4. Results and discussion

Each of the individual samples was analysed in triplicate, and the resulting data used to generate error bars showing two standard deviations either side of the mean. As can be seen in the [Figs. 1, 3, 6 and 8](#) the error bars are typically small for the techniques, indicating consistent and reproducible results. The three-stage fitting of adsorption isotherms is discussed below.

The most appropriate models for fitting the results are the D–R model, mentioned below, and the ARIAN bilayer model. However, the authors of the ARIAN model fitted it only to stage III of their data. Fits to the whole range of our data did not, in general, properly represent the stages we observed, [Figs. S6–S13](#). Therefore, as explained above, we used the Langmuir isotherm [21] (Eq. (4)) as a means of smoothing our data, and of calculating asymptotes. Aqueous concentrations (c_e) were plotted against the aqueous phase concentrations divided by adsorbed concentration (q_e). From the line of best fit it was then possible to calculate the maximum amount adsorbed (q_{max}) and the equilibrium constant (K), [Table S2](#):

$$\frac{c_e}{q_e} = \frac{c_e}{q_{max}} + \frac{1}{Kq_{max}} \quad (4)$$

Due to the presence of both hydrophilic and hydrophobic mineral surfaces, and the colloidal nature of the adsorbent, it was expected that a single Langmuir isotherm would be inadequate for describing the adsorption process. Visual inspection of [Figs. 1, 2, 6 and 7](#) confirms that there are distinct adsorption stages.

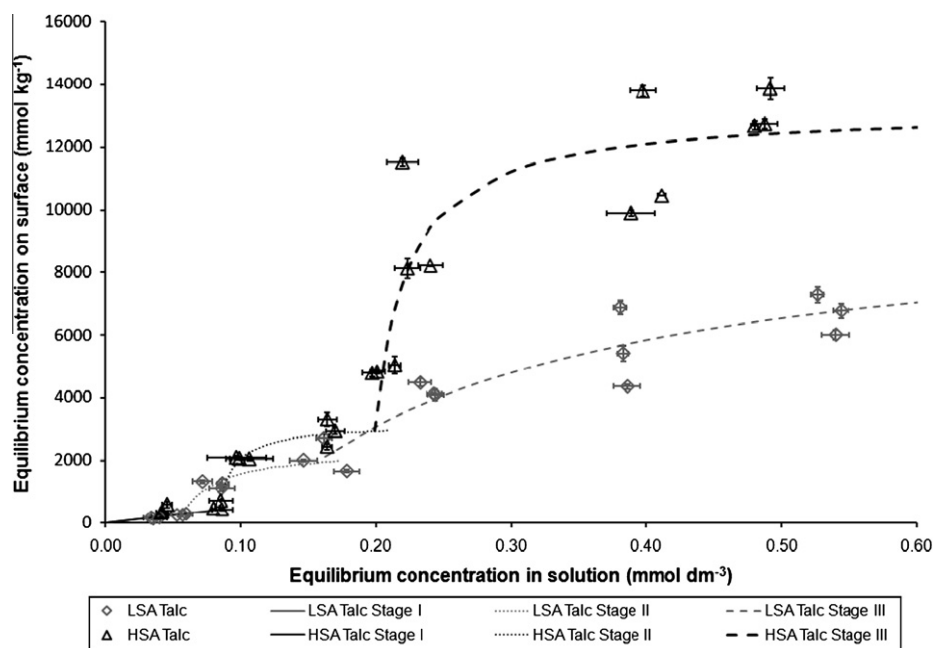


Fig. 1. Adsorption of the fatty acid ester defoamer onto LSA and HSA talc.

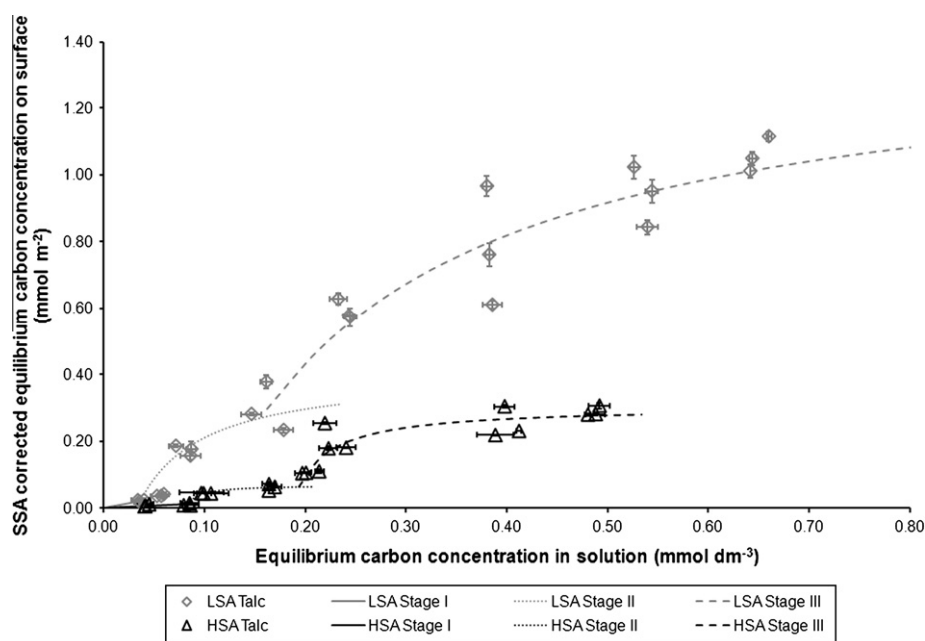


Fig. 2. Adsorption of the fatty acid ester defoamer onto LSA and HSA talc, after correction for specific surface area.

The D–R adsorption energies calculated using Eq. (1) are all less than 200 J mol^{-1} , Table S3, implying that physisorption [24] is the adsorption mechanism for forming a sticky monolayer.

4.1. Adsorption of fatty acid ester defoamer on mineral surfaces

The carbon concentrations, as a proxy for the concentration of the fatty acid ester defoamer, adsorbed onto LSA and HSA talc are shown on a mass basis and as a function of ester defoamer remaining in solution in Fig. 1 and on a surface area basis in Fig. 2. The figures show that HSA talc adsorbed more efficiently

than LSA talc per unit mass, Fig. 1, but less efficiently per unit surface area, Fig. 2.

Fig. 3 shows the extent of adsorption of fatty acid ester defoamer onto the two types of MCC. The results show that the HSA MCC does not adsorb the sticky as well, per unit mass, as the LSA MCC. The LSA MCC range could not be extended in respect to adsorbate, due to visible deposits forming on glassware at concentrations greater than 0.5 g dm^{-3} .

An explanation for the adsorption stages encountered for talc and the MCC can be suggested using knowledge of the structure of a fatty acid ester molecule, which we suggest forms a dimer

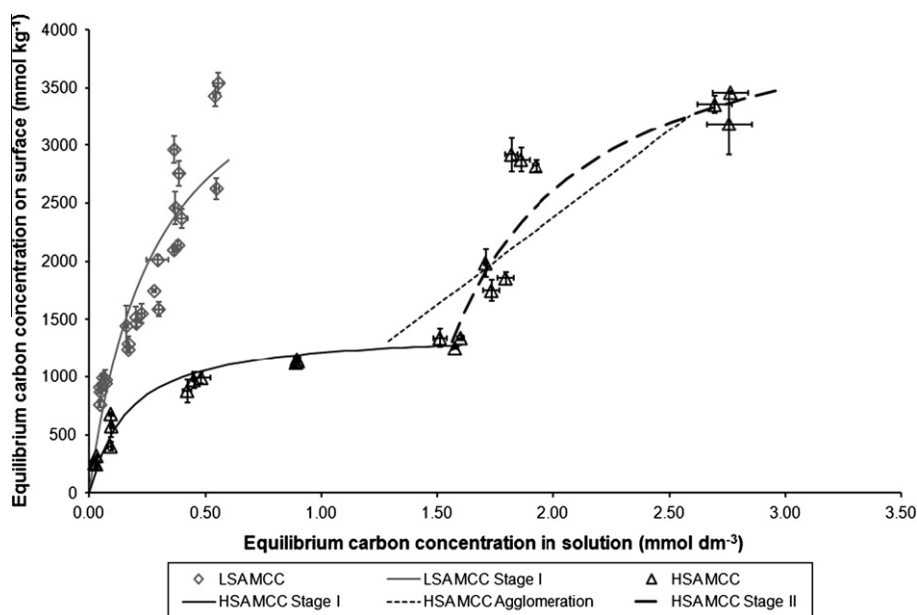


Fig. 3. Adsorption of fatty acid ester defoamer onto LSA MCC and HSA MCC.

when present in water to increase the stability of the molecule [39,40].

In Figs. 1 and 2 the adsorption of the fatty acid ester species onto talc has been divided into three distinct stages; each of the stages has a different adsorption mechanism proposed due to the heterogeneity of talc and fatty acid ester defoamer. Before adsorption can occur, we suggest that hydroxide groups may leave the edges of the talc and go into solution. Magnesium hydroxide has an alkaline dissociation constant (pK_b) of 2.60 at 25 °C [41]. However, it is also possible for the magnesium hydroxide to be protonated by a hydronium ion forming OH_2^+ , which is more likely in acidic conditions [42] similar to how a silica-gel would adsorb [43]. For both mechanisms a positively charged species is available for adsorption, either Mg^{2+} or OH_2^+ , so the mechanism will not change. The first adsorption stage occurs over a limited aqueous concentration range with no significant adsorption for either talc grade. We suggest the initial adsorption stage uses a dimeric form of the fatty acid ester defoamer adsorbing on the hydrophilic edges of the talc, Fig. 4.

The second stage involves the adsorption of the hydrophobic ends of single (un-dimerised) molecules onto the hydrophobic regions of the surface to form a sticky monolayer. As explained previously, the HSA talc has a higher aspect ratio and, therefore, a higher ratio of hydrophobic surface area relative to hydrophilic surface area for a given particle size [31,33]. The higher stage II adsorption for HSA talc shown in Fig. 2 supports the assertion that stage II is predominantly occurring at the hydrophobic surfaces, which dominate in terms of surface area, Fig. 4. We suggest that the third adsorption stage involves the formation of an additional monolayer of appropriately orientated fatty acid ester defoamer molecules, Fig. 4. We propose only one additional monolayer as the high relative permittivity of water would quench further adsorption [44].

Fig. 3 shows the adsorption isotherms for LSA MCC and HSA MCC. Adsorption onto the LSA MCC follows a single Langmuir isotherm, implying monolayer adsorption. The HSA MCC results show two distinct stages, which the data suggest is monolayer adsorp-

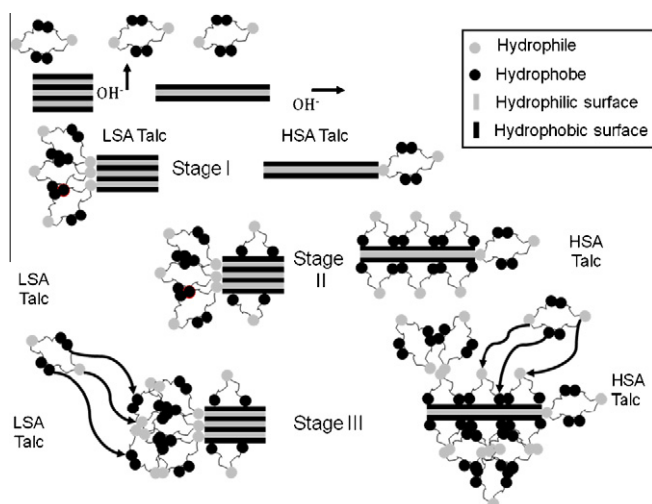


Fig. 4. Schematic showing a possible mechanism for the adsorption of a fatty acid ester defoamer onto LSA and HSA surface area talc, respectively. For clarity the size of the ester molecule has been enlarged relative to the talc.

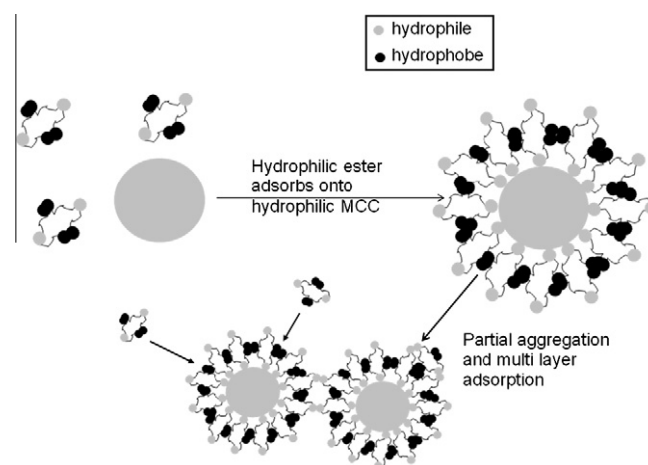


Fig. 5. Schematic showing proposed adsorption mechanism for a fatty acid ester defoamer onto modified calcium carbonate (MCC) or a completely hydrophilic mineral. For clarity the size of the ester molecule has been enlarged relative to the MCC.

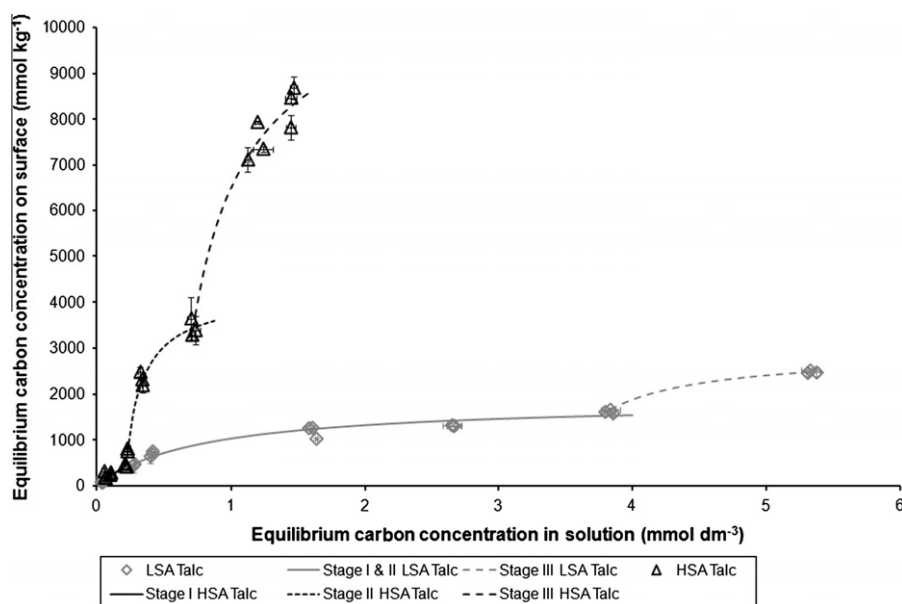


Fig. 6. Adsorption of acrylic acid ester copolymer onto LSA and HSA talc.

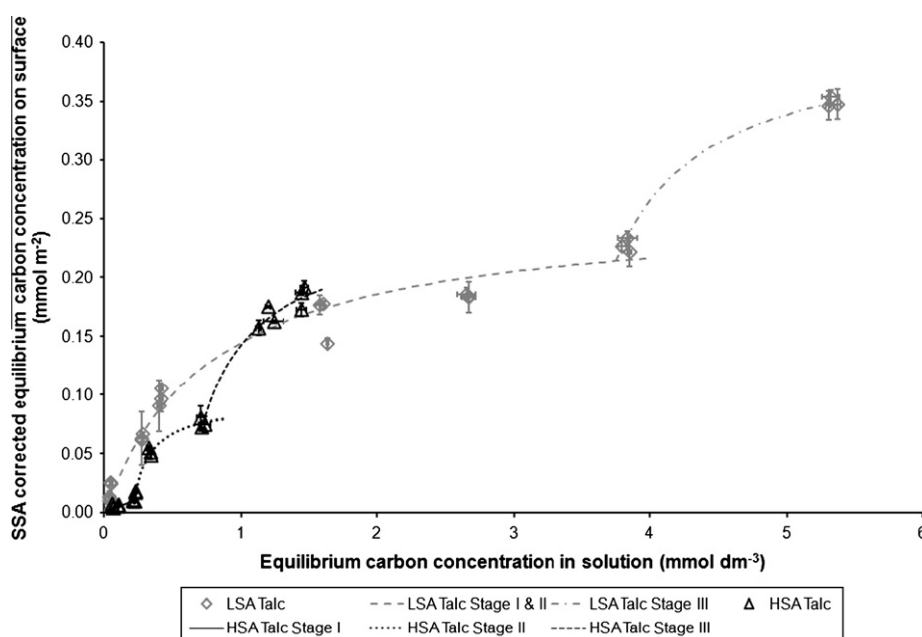


Fig. 7. Adsorption of an acrylic acid ester copolymer onto LSA and HSA-talc corrected for the specific surface area of the talc.

tion, Fig. 5, followed by multi-layer adsorption and partial aggregation of the mineral-with-adsorbent species. The fatty acid ester molecules are supplied with surfactant, so will not aggregate with each other. The HSA MCC is dispersed using polyacrylate, and the carbon content of the polyacrylate is taken into consideration during data analysis. The LSA MCC has no surfactant, but the experiment could not be carried out at higher concentrations, as explained previously.

4.2. Adsorption of acrylic acid ester copolymer on mineral surfaces

Fig. 6 shows the adsorption of the acrylic acid ester copolymer onto the LSA and HSA talc. As expected, the HSA talc is significantly better per unit mass of talc at adsorbing the acrylic acid ester copolymer than the LSA talc. Fig. 7 shows the acrylic acid ester

copolymer adsorption after correction for specific surface area. Fig. 8 shows the adsorption of the acrylic acid ester copolymer onto the MCCs, with a greater adsorption per unit mass onto the LSA MCC.

In Figs. 6 and 7 the first stage results show that adsorption is greater for the LSA talc than HSA talc, suggesting that adsorption is occurring at the hydrophilic edges, Fig. 9. The HSA talc results exhibit two distinct stages of adsorption; the first stage is hydrophilic adsorption, and the second stage is hydrophobic adsorption, because HSA talc adsorbs more than the LSA talc. The third stage is assumed to be adsorption of an additional monolayer of sticky.

In Fig. 8 the results show adsorption onto the LSA MCC, and the first and second stage of the adsorption onto HSA MCC can be usefully fitted using Langmuir relations. During the second HSA MCC

stage, the turbidity increased, which implies partial aggregation, (Eq. (3)). The Langmuir isotherm allows the calculation of the maximum adsorption values for each adsorption stage. The acrylic acid ester copolymer adsorbing onto HSA MCC gives maximum adsorption values of $q_{\max,1} = 8\ 050\ \text{mmol kg}^{-1}$ and $q_{\max,2} = 12\ 200\ \text{mmol kg}^{-1}$ for the 1st and 2nd stage, respectively. For both stages of adsorption to be following Langmuir behaviour, $q_{\max,2}$ would need to be at least double $q_{\max,1}$. Some multi-layer adsorption does occur, but the absence of this clear relationship between $q_{\max,1}$ and $q_{\max,2}$ suggests that aggregation takes place during the 2nd stage, Fig. 10.

Some of the differences between the LSA and HSA MCC can be explained by the differences in particle size. When a sticky particle is close to the size of the mineral particle the adsorption capacity decreases, as fewer sticky particles need to be adsorbed to reach saturation of the mineral particle. As the particle reaches saturation more quickly there will be more mobile sticky in suspension promoting aggregation at higher concentrations.

4.3. pH, conductivity, zeta potential and turbidity

The pH of 7.40 of the suspension at the beginning of the experiment remained constant to within 0.51 on adsorption of the fatty acid ester defoamer. For adsorption of the acrylic acid ester copolymer, it remained constant to within 0.14 from the starting pH of 7.32. The conductivity decreased for both sticky suspensions after adsorption, in line with fewer charged particles remaining in suspension. For the fatty acid ester defoamer the conductivity decreased from $1034\ \mu\text{S cm}^{-1}$ before adsorption to $812\text{--}826\ \mu\text{S cm}^{-1}$ after adsorption, and the acrylic acid ester copolymer decreased from $1133\ \mu\text{S cm}^{-1}$ before adsorption to $958\text{--}984\ \mu\text{S cm}^{-1}$ after adsorption. The reduction in the electrical conductivities of the solution after the adsorption supports the assumption that charged species were removed from solution or suspension.

The zeta potential results in the Supplementary information, Fig. S5, for both sticky types show differences between the talc grades. For the fatty acid ester defoamer the zeta potential of the remaining unadsorbed species was more negative than the starting species, showing that the less stable species have been adsorbed and the more stable species left in suspension, as might be expected.

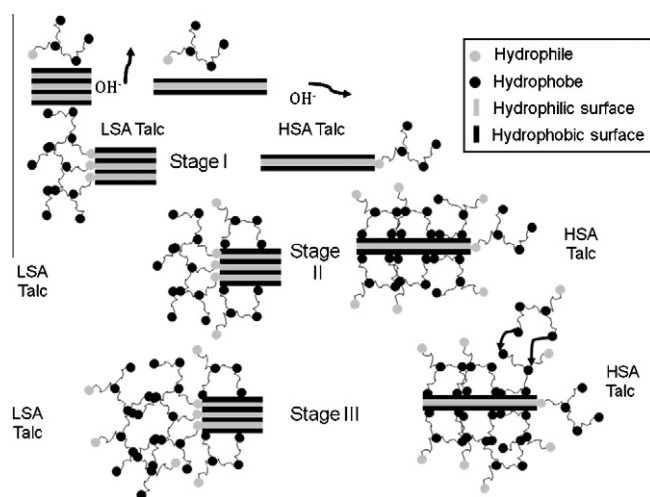


Fig. 9. Schematic showing proposed adsorption mechanism for an acrylic acid ester copolymer onto LSA and HSA talc. For clarity the size of the ester molecule has been enlarged relative to the talc.

The zeta potential changes for the acrylic acid ester copolymer adsorptions were different for the two talc grades. The zeta potential of the supernatant above the LSA talc did not change significantly after adsorption. The zeta potential of the HSA talc is slightly less negative. This implies that for the LSA talc, equal quantities of anionic and cationic species were removed by adsorption, whereas the HSA talc preferentially adsorbed more anionic species (i.e. species more negatively charged at their shear planes). This deduction is in accord with the differences in adsorption characteristics shown in Fig. 6. HSA talc shows three distinct stages. However, because of the adsorption of both anionic and cationic species onto the LSA talc, stages I and II are merged.

The interpretation of the adsorption onto the two modified calcium carbonate (MCC) grades is more complicated. It can be seen that they behave differently towards the defoamer (on the left of Fig. S5) and the copolymer. The differences suggest that there must be both cationic and anionic adsorption sites on MCC. The defoamer adsorbs preferentially onto the anionic sites of LSA MCC, leaving the supernatant with a more negative zeta potential,

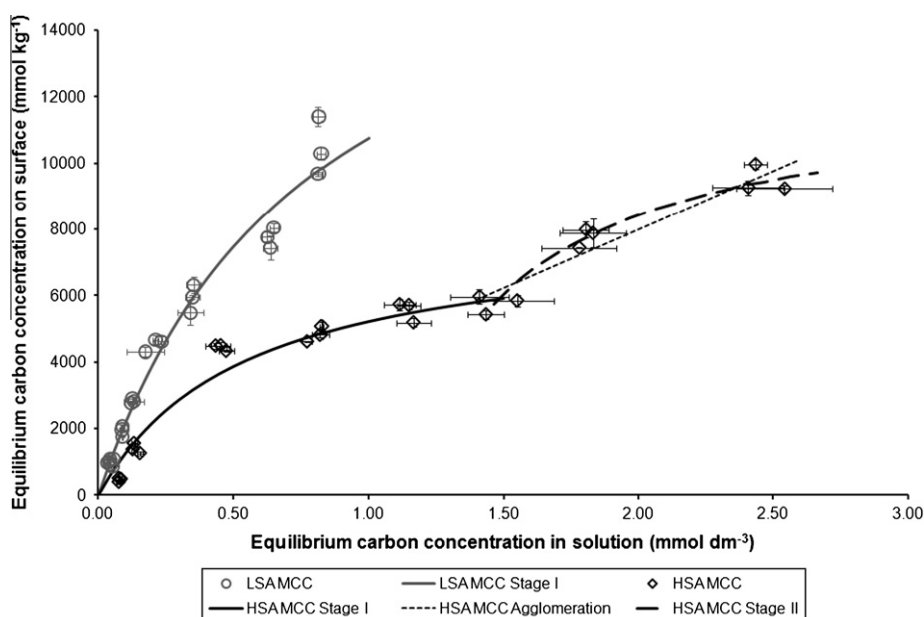


Fig. 8. Adsorption of an acrylic acid ester copolymer onto LSA MCC and HSA MCC.

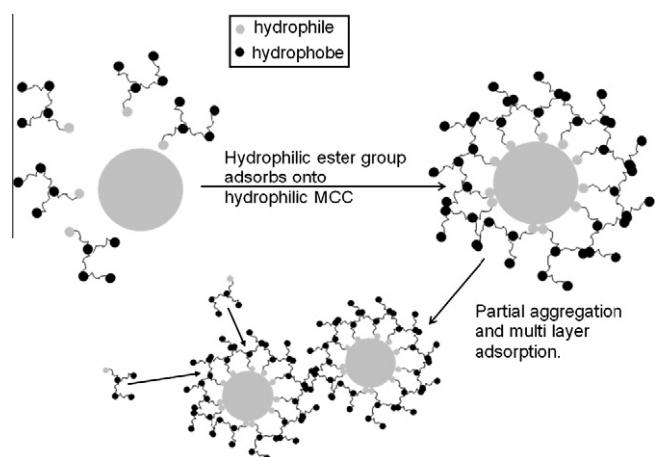


Fig. 10. Schematic showing proposed adsorption mechanism for acrylic acid ester copolymer onto modified calcium carbonate or a hydrophilic mineral. For clarity the size of the ester molecule has been enlarged relative to the MCC.

whereas the copolymer adsorbs preferentially onto the cationic sites, leaving the supernatant with a lower (more positive) zeta potential than at the start of the experiment. Similarly, the defoamer adsorbs preferentially onto the anionic sites of HSA MCC, and the copolymer adsorbs even more preferentially onto the cationic sites of the HSA MCC. The conductivity changes confirm that charged species were removed from suspension during the experiment, but do not indicate whether the species are anionic or cationic.

The aggregation of mineral and sticky suspension is supported by turbidity changes during the adsorption experiment. For the higher sticky concentration experiments, the turbidity for the HSA MCC with both model stickies increased during the thirty minutes the suspension was reaching equilibrium before it was centrifuged. During this time, by mass conservation, the term ν in Eq. (1) will remain constant. Therefore, an increase in turbidity must have been caused by an increase in the volume v of particles, indicating aggregation. However, this aggregation is slight, at only 1.3–1.4%. By contrast, no turbidity change, and hence no aggregation, was observed for the LSA MCC. As stated previously, the LSA MCC experiment could not be carried out at the higher end of the sticky concentration because of adsorption onto the glassware. This provides a likely explanation of why no aggregation was seen.

5. Conclusions

This investigation used commercially available suspensions of model stickies, with undefined surfactants, in a laboratory system to determine adsorption onto mineral surfaces representing an *in situ* industrial environment. The results suggest multistage adsorption. Multi-step Langmuir isotherms were used to describe adsorption onto different mineral systems, comparing the hydrophobic planar and hydrophilic edge surfaces of talc, and hydrophilic MCCs. Possible adsorption mechanisms have been proposed for sticky systems, which explain the results. The most efficient adsorbent of the fatty acid ester defoamer was the HSA talc per unit mass, due to the presence of a high surface area of hydrophobic surfaces. The most efficient at adsorbing the acrylic acid ester copolymer was the LSA MCC. Additionally, the use of the chosen adsorbates enabled a description of the MCC surface charge balance to be derived in terms of coexisting anionic and cationic charge.

The results reported used a novel proxy method to allow the construction of adsorption isotherms of commonly found colloidal

contaminants in a paper recycling environment, which have significant financial implications to the industry. The proxy method has a wide applicability for the study of the complex adsorption systems.

Acknowledgments

The authors wish to acknowledge Omya Development AG, Switzerland, and HEIF 3 for funding the project. Omya Development AG is thanked for supporting cooperation between the University of Plymouth and its industrial Mineral and Surface Chemistry R&D.

Appendix A. Supplementary material

Supplementary data associated with this article can be found, in the online version, at [doi:10.1016/j.jcis.2010.07.062](https://doi.org/10.1016/j.jcis.2010.07.062).

References

- [1] M.R. Doshi, Prog. Pap. Recycl. 1 (1991) 54–63.
- [2] M. Douek, X.Y. Guo, J. Ing, Recycl. Symp. (1997) 313–330.
- [3] D.R. Jones, J.W. Fitzhenry, Pulp. Pap. 77 (2003) 28–33.
- [4] M.R. Doshi, J.M. Dyer, Pap. Recycl. Chal. 3 (1998) 195–233.
- [5] D.T. Nguyen, Tappi J. 81 (1998) 143–151.
- [6] I.M. Hutten, R. Diaz, M.K. Roberts, C. Jeffrey, S. Banerjee, Tappi J. 80 (1997) 193–197.
- [7] C.R. Olson, M.K. Letscher, Appita J. 45 (1992) 125–130.
- [8] H. Onusseit, Resour. Conserv. Recycl. 46 (2006) 168–181.
- [9] T. Delagoutte, Prog. Pap. Recycl. 17 (2008) 9–16.
- [10] F. Benecke, D. Gantenbein, J. Schoelkopf, P.A.C. Gane, T. Gliese, Nord. Pulp Pap. Res. J. 24 (2009) 219–224.
- [11] T. Delagoutte, Prog. Pap. Recycl. 15 (2005) 31–41.
- [12] W. Spiess, K. Renner, Wochenbl. Papierfabr. 132 (2004) 1002–+.
- [13] O.U. Heise, M. Kemper, H. Wiese, E.A. Krauthauf, Tappi J. 83 (2000) 73–79.
- [14] M. Kemper, Int. J. Miner. Process. 56 (1999) 317–333.
- [15] K.R. Rogan, Colloid Polym. Sci. 272 (1994) 82–98.
- [16] M. Douek, L.H. Allen, J. Pulp Pap. Sci. 17 (1991) J171–J177.
- [17] L.H. Allen, M. Douek, J. Pulp Pap. Sci. 19 (1993) J131–J136.
- [18] B. Holmbom, A. Sundberg, Wochenbl. Papierfabr. 131 (2003) 1305–1311.
- [19] L.J. Vähäsalo, B.R. Holmbom, Appita J. 59 (2006) 280–284.
- [20] M.R. Doshi, Prog. Pap. Recycl. 13 (2003) 44–53.
- [21] I. Langmuir, J. Am. Chem. Soc. 40 (1918) 1361–1403.
- [22] J.C. Igwe, A.A. Abia, Afr. J. Biotechnol. 5 (2006) 1167–1179.
- [23] M.J. Horsfall, A.I. Spiff, Electron. J. Biotechnol. 7 (2004).
- [24] S. Motoyuki, Adsorption Engineering, Elsevier, Japan, 1990.
- [25] S. Paria, K.C. Khilar, Adv. Colloid Interface Sci. 110 (2004) 75–95.
- [26] R. Zhang, P. Somasundaran, Adv. Colloid Interface Sci. 123–126 (2006) 213–229.
- [27] B. Samiey, S. Golestan, Cent. Eur. J. Chem. 8 (2010) 361–369.
- [28] G.M.S. El Shafei, N.A. Moussa, J. Colloid Interface Sci. 238 (2001) 160–166.
- [29] P. Atkins, J. de Paula, Atkins' Physical Chemistry, Oxford University Press, Trento, Italy, 2002.
- [30] S. Brunauer, P.H. Emmett, E. Teller, J. Am. Chem. Soc. 60 (1938) 309–319.
- [31] V. Wallqvist, P.M. Claesson, A. Swerin, J. Schoelkopf, P.A.C. Gane, Langmuir 23 (2007) 4248–4256.
- [32] M. Sakai, T. Yanagisawa, A. Nakajima, Y. Kameshima, K. Okada, Langmuir 25 (2008) 13–16.
- [33] V. Wallqvist, P.M. Claesson, A. Swerin, J. Schoelkopf, P.A.C. Gane, Colloids Surf., A 277 (2006) 183–190.
- [34] C.J. Ridgway, P.A.C. Gane, J. Schoelkopf, Trans. Por. Med. 63 (2006) 239–259.
- [35] E.S. Badr, E.P. Achterberg, A.D. Tappin, S.J. Hill, C.B. Braungardt, Trends Anal. Chem. 22 (2003) 819–827.
- [36] X. Pan, R. Sanders, A.D. Tappin, P.J. Worsfold, E.P. Achterberg, J. Autom. Methods Manage. Chem. 4 (2005) 240–246.
- [37] D.M. Lawler, in: A. Townshend (Ed.), Turbidimetry and nephelometry, Encyclopedia of Analytical Science, Academic Press, 1995, pp. 5289–5297.
- [38] R.J. Hunter, Zeta Potential in Colloid Science: Principles and Applications, Academic Press Ltd., East Kilbride, 1981.
- [39] M. Patujej, M. El Fray, Polimery 54 (2009) 611–617.
- [40] M.R. Silva, A.J.F.N. Sobral, J.A. Silva, A.C. Santos, S.M. Melo, A.M. Beja, J. Chem. Crystallogr. 37 (2007) 695–698.
- [41] CRC Handbook of Chemistry and Physics, CRC Press, Inc, Florida, USA, 2004.
- [42] A. Guyard, C. Daneault, B. Chabot, Nord. Pulp. Pap. Res. J. 21 (2006) 620–628.
- [43] S.K. Parida, B.K. Mishra, Colloids Surf., A: Physicochem. Eng. Asp. 134 (1998) 249–255.
- [44] S.B. Jones, D. Or, J. Non-Cryst. Solids 305 (2002) 247–254.
- [45] P. Somasundaran, S. Krishnakumar, Colloids Surf., A: Physicochem. Eng. Asp. 123–124 (1997) 491–513.